Connections between climate, food limitation, and carbon cycling in abyssal sediment communities

Henry A. Ruhl[a,b,1], Jacob A. Ellena[b], and Kenneth L. Smith, Jr.[b]

[a]National Oceanography Centre, Southampton, Ocean Biogeochemistry and Ecosystems (DEEPSEAS Group), Southampton, SO14 3ZH, United Kingdom; and [b]Monterey Bay Aquarium Research Institute, 7700 Sandholdt Road, Moss Landing, CA 95039

Diverse faunal groups inhabit deep-sea sediments over much of Earth's surface, but our understanding of how interannual-scale climate variation alters sediment community components and biogeochemical processes remains limited. The vast majority of deep-sea communities depend on a particulate organic carbon food supply that sinks from photosynthetically active surface waters. Variations in food supply depend, in part, on surface climate conditions. Proposed ocean iron fertilization efforts are also intended to alter surface production and carbon export from surface waters. Understanding the ecology of the abyssal sediment community and constituent metazoan macrofauna is important because they influence carbon and nutrient cycle processes at the seafloor through remineralization, bioturbation, and burial of the sunken material. Results from a 10-year study in the abyssal NE Pacific found that climate-driven variations in food availability were linked to total metazoan macrofauna abundance, phyla composition, rank-abundance distributions, and remineralization over seasonal and interannual scales. The long-term analysis suggests that broad biogeographic patterns in deep-sea macrofauna community structure can change over contemporary timescales with changes in surface ocean conditions and provides significant evidence that sediment community parameters can be estimated from atmospheric and upper-ocean conditions. These apparent links between climate, the upper ocean, and deep-sea biogeochemistry need to be considered in determining the long-term carbon storage capacity of the ocean.

biogeochemistry | community structure | deep sea | ecology | macrofauna

Appreciating how climate can influence deep-sea communities and biogeochemical cycles is essential in evaluating how they may vary in the future. Current evidence suggests that climate change is resulting in significant alterations of oceanographic conditions worldwide including increased sea-surface temperatures, stronger stratification, and increased acidity (1, 2). The changing climate will likely also impact net primary production (1, 3–7) and the export of particulate organic carbon (POC) to the deep sea. Life on the seafloor depends upon this sinking POC and has a fundamental influence on the amount of carbon and nutrients that are remineralized or buried there. Ocean iron fertilization plans also project increases in surface production and POC export from surface waters, but fertilization impacts are poorly constrained (8, 9), especially for the deep-sea sediment community.

Detailed studies of macrofauna, a major component of the sediment community, have been conducted at various locations and depths worldwide and have generally found higher abundances below areas with greater surface production (10–16). Abyssal food supply varies with distance from shore, depth, and surface productivity at basin scales. Previous studies that covered adequate spatial areas, however, understandably lacked long-term temporal perspective. Most spatial studies have effectively compared sediment fauna abundance across a gradient of spatial variation in surface production (10–16). For example, a metaanalysis of samples collected from 1961 to 1985 in the western North Atlantic found that the principal pattern of macrofauna abundance was related to depth-corrected POC flux as determined from the more modern sea-viewing wide field-of-view sensor (SeaWiFS) ocean color data (13). Analysis of patterns in body size distributions have also found a decrease in average body size with increasing depth and/or decreasing food availability (12, 17, 18).

Time-series research of abyssal communities has been more limited. Previous time-series studies have comprehensively described deep-sea community collapses that occurred in synchrony to glaciations (19) and centennial-scale climate variations since the time of the last glacial maximum (20). Contemporary research has examined macrofauna abundance in the northeast (NE) Atlantic over six times from 1996 to 1998 and the results showed varying responses in taxon-specific abundances to the seasonally varying food supply at the study site (21). Two studies in the North (N) Pacific also found seasonal variations in the abundance of several macrofauna taxa from June 1989 to February 1991 in the NE Pacific [Station (Sta.) M] (22) and over a 14-month period in the central North Pacific (Station ALOHA) in 1997 and 1998 (23). Seasonal variations have also been found in other faunal groups such as foraminifera (24). Previous investigations have been revealing, but assessment of contemporary time-series data over interannual scales is required to determine whether year-to-year changes in surface conditions and food supply do indeed lead to interannual changes in the macrofauna community and ultimately to abyssal carbon cycling.

The results presented here illustrate how climate-forced POC fluxes are correlated to broad-scale fluctuations in sediment communities and carbon cycling at abyssal depths. The northern oscillation index (Fig. 1A) (NOI) (25) El Niño indicator was previously correlated to POC flux to the seafloor (Fig. 1B) at Sta. M (26). La Niña periods of the El Niño southern oscillation (ENSO) were related to increased upwelling, cooler sea-surface temperatures, and greater net primary production, export, and abyssal POC flux (26). Here we describe how seasonal and longer-term variations in POC flux were correlated to abyssal metazoan macrofauna abundance, community composition and structure, and carbon remineralization by using data from a 10-year study conducted at a northeast Pacific study site, Station M (34°50′N, 123°00′W, 4,100-m depth).

Sediment community dynamics were examined using a series of 95 free vehicle grab respirometer (FVGR) (27) samples collected during 39 deployments from 1989–1998 at Station M. Sediment community oxygen consumption (SCOC; an indicator of carbon remineralization and food demand) measurements were made during each deployment of the FVGR in up to four grab chambers
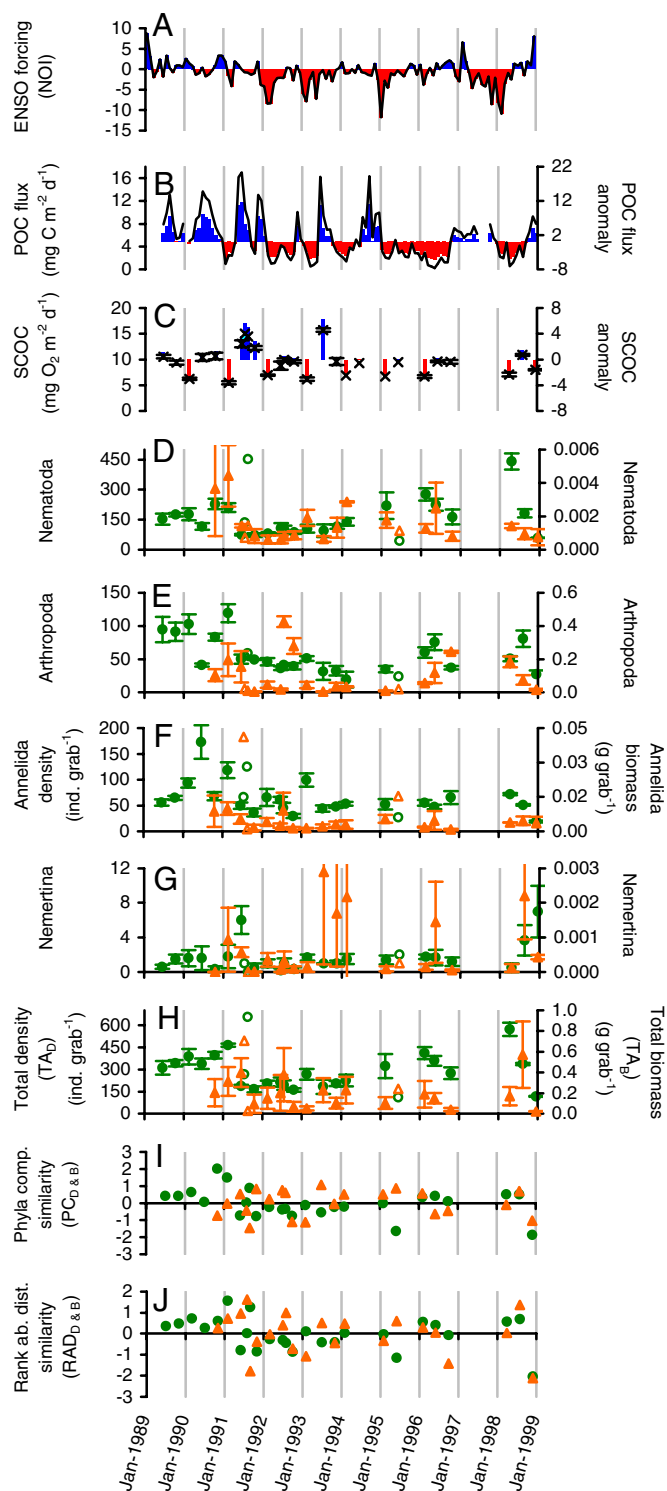

Fig. 1. (A) Monthly northern oscillation index (NOI) with monthly anomaly in blue and red; (B) monthly POC flux composite (SI) to 50 m above bottom with monthly anomaly in blue and red; (C) monthly SCOC (×) with monthly anomaly in blue and red; density (circles) and wet-weight biomass (triangles) for the top four most abundant metazoan macrofauna phyla (D) Nematoda, (E) Arthropoda, (F) Annelida, (G) Nemertina, (H) total density (TA_D, circles), and total biomass (TA_B, triangles). The biomass data are only available beginning in October 1990. Solid symbols have standard error bars and open symbols represent single grab samples. (I) Monthly macrofauna phyla-composition similarity based on both density (PC_D, circles) and biomass data (PC_B, triangles), and (J) RAD similarity based on both density (RAD_D, circles) and biomass data (RAD_B, triangles). Higher phyla composition and RAD similarity MDS x-ordinates are aligned with higher density and biomass.

each enclosing a 413-cm^2 area of seabed and the top 15 cm of sediment. After respiration incubations of ~2 days these grabs also collected the enclosed sediment. The recovered samples were sieved on a 300-μm screen and the retained metazoan taxa were sorted to phylum, counted, and wet weights determined (22). Because abundances are for those animals retained on a 300-μm screen, there is under sampling of individuals smaller than the screen size, particularly for the phylum considered here with the smallest average body size, the Nematoda.

Six parameters were used to describe the metazoan macrofauna community dynamics. Using density ($_D$) data we calculated total abundance (TA$_D$), and the Bray-Curtis similarity multidimensional scaling (MDS) x-ordinates of phyla composition (PC$_D$) and rank-abundance distribution (RAD$_D$)(Fig. 1 *H–J*). Similarly biomass ($_B$) data were also used to determine total abundance (TA$_B$), the phyla composition (PC$_B$), and rank-abundance distribution (RAD$_B$) similarities. The influence of the food supply on the studied macrofauna was evaluated by cross-correlating the faunal parameters to abyssal POC flux from sediment-trap and model estimated data using the Spearman-rank correlation [Fig. 1*B*, supporting information (SI)].

Monthly and yearly fluctuations in abyssal POC fluxes had marginal-to-significant ($P < 0.10$ to $P < 0.05$) correlations to all six community parameters (TA$_D$, TA$_B$, PC$_D$, PC$_B$, RAD$_D$, and RAD$_B$) with higher fluxes linked to higher TA$_D$ and TA$_B$ (Figs. 1–3, Table 1). At the community level TA$_D$ was significantly correlated ($P < 0.01$) to PC$_D$ and RAD$_D$ with higher TA$_D$ associated with decreased evenness. Among the dominant phyla the monthly Arthropoda densities had a significant correlation to POC fluxes as did the biomasses of the Arthropoda, Nematoda, and Nemertina ($P < 0.05$). A set of yearly multiple regressions using the NOI and abyssal POC flux as inputs accounted for 80–90% of the variation in TA$_D$, PC$_D$, and RAD$_D$ (Fig. 3*E*). Similar biomass-based regressions were not significant and analogous regressions on a monthly basis accounted for <50% of the observed variation with mixed significance.

The temporal lags between food supply and the six macrofauna community parameters increased with the spatiotemporal scale found in earlier studies at Sta. M (26–29). Changes in the NOI were previously found to lead to changes in the Sta. M food supply after ~6 months (26). Cross-correlations here indicated that peaks in POC flux were followed by fluctuations in TA$_D$, PC$_D$, and RAD$_D$ after ~3–4 months for density-based parameters and 7–8 months for the biomass-based parameters TA$_B$, PC$_B$, and RAD$_B$ (Table 1). The peak temporal lags between the NOI and each of the six community parameters were significantly correlated to the sum of the component temporal lags between NOI and POC flux and between POC flux and the community parameters ($P = 0.04$, Table 1, SI). The interval between shifts in food supply and macrofauna densities reported here were generally shorter than those found for the larger mobile megafauna at Sta. M (28, 29), which is consistent with the expectation that smaller fauna respond more quickly to food inputs. Although all cases are not significant, a consensus emerged indicating links between climate, food supply, and the metazoan community.

Transitions from larger to smaller body size dominance during lower food supplies also confirm hypotheses from spatial studies (12, 17, 18) that food availability influences interspecific body-size distributions of deep-sea macrofauna. Overall the monthly average biomass (per capita TA$_B$) correlated positively with POC flux with a lag of ~7 months ($r_s = 0.60$, $n = 21$, $P = 0.004$)(Fig. 2*B*). Using data grouped by year increases in POC flux were followed by significant increases in average body size ~1 year later ($r_s = 0.94$, $n = 6$, $P = 0.005$). These correlations, however, can be determined by inter- and intraspecific body size-to-abundance relationships. If body size distributions between taxa were determined by food availability, then rank
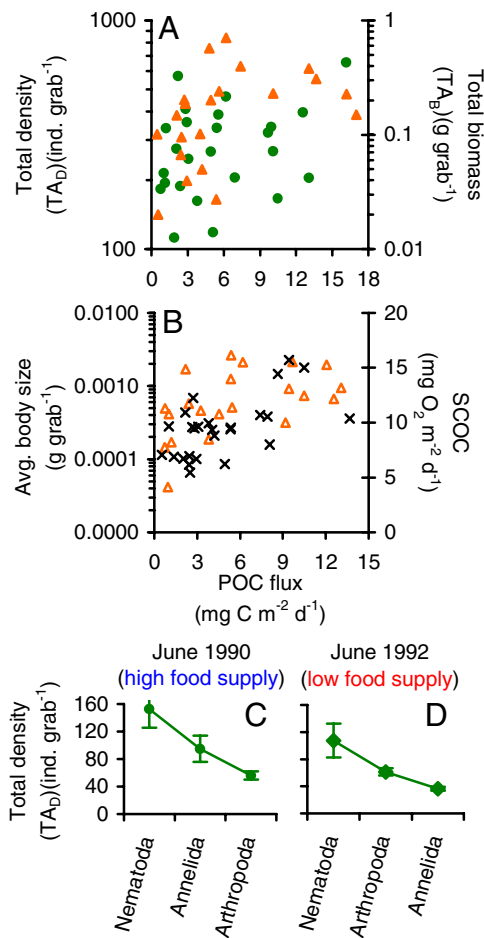
ECOLOGY

Fig. 2. (*A*) Scatter plots of total density (TA$_D$, circles) and total biomass (TA$_B$, triangles) vs. observed POC flux using time lags presented in Table 1. (*B*) Average body size (triangles) and SCOC (crosses) vs. POC flux based on time lags in Table 1. Body size distributions for the top three most abundant phyla during an example higher-than-average flux period in June 1990 (*C*), and a lower-than-average flux period in June 1992 (*D*) with standard error bars shown. The Annelida typically were higher in abundance than the Arthropoda (*P* < 0.05, *SI*).

switches from smaller to larger taxa dominance might even be associated with higher food availability over monthly timescales. Here the top three phyla in TA$_D$ were Nematoda, with the smallest per capita biomass, followed by the sequentially larger Arthropoda and Annelida. Nematodes uniformly had the highest TA$_D$, but the Arthropoda and Annelida exhibited several monthly switches in TA$_D$ rank (e.g., Fig. 2 *C* and *D*). The Annelida, which were generally larger in size, had higher densities when food supplies were elevated and the Arthropoda, which were smaller on average, were more dense during lower food fluxes [analysis of similarity (ANOSIM), *P* = 0.03]. The site-specific nature of the rank switches also reduces the confounding influences of changes in sediment grain size and seafloor hydrodynamic conditions often associated with comparing body-size distributions between different study areas.

Density measures had low overall synchrony to biomass at the community level, but the Nematoda, Annelida, and Nemertina had significant covariation of density and biomass on a monthly basis (Fig. 1 *D*, *F*, and *G*; *SI Text*). One possible explanation for low overall synchrony between density and biomass is that after a pulse of POC flux, any increases in reproduction and/or recruitment led to more small individuals on average that subsequently grew larger after a few months with lesser impor-
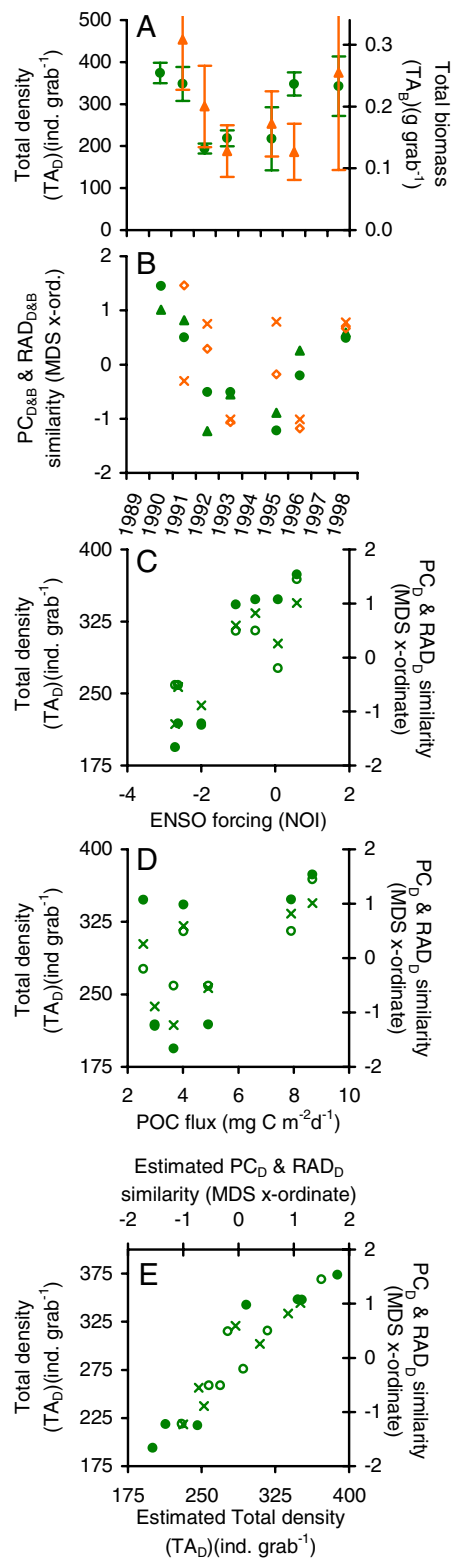

Fig. 3. Yearly metazoan macrofauna (*A*) TA$_D$ (circles) and TA$_B$ (triangles) with standard error bars shown, (*B*) PC$_D$ (circles) and RAD$_D$ similarity (triangles), and PC$_B$ (×) and RAD$_B$ (diamonds); (*C*) total density, PC$_D$, and RAD$_D$ over observed yearly ENSO forcing conditions as represented by the NOI; (*D*) TA$_D$ (circles) and PC$_D$ (○) and RAD$_D$ (×) similarity over observed yearly POC fluxes to 50 mab; (*E*) regression model [*y* = POC(*a*) + NOI(*c*) + intercept] estimated density-based community parameters TA$_D$ (circles), and PC$_D$ (○) and RAD$_D$ similarity (×) (model fits evaluated using the *F*-test: TA$_D$, *n* = 7, *r*^{2} = 0.90, *P* = 0.011; PC$_D$, *n* = 7, *r*^{2} = 0.80, *P* = 0.038; and RAD$_D$, *n* = 7, *r*^{2} = 0.85, *P* = 0.024).

Table 1. Peaks in Spearman-rank cross correlations (r_s) with resulting P-values comparing the density and biomass-based total abundance (TA_D and TA_B), and phyla composition (PC_D and PC_B) and rank-abundance distribution (RAD_D and RAD_B) MDS x-ordinates of similarity to POC flux and the NOI over monthly timescales with the community parameter lagging the resource or environment variable by the number of months shown and yearly correlations between the above community parameters

Macrofauna parameters	Monthly								Yearly					
	POC flux				NOI				POC flux			NOI		
	Lag	n	r_s	P	Lag	n	r_s	P	n	r_s	P	n	r_s	P
Density-based														
Phyla comp. sim. (PC_D, MDS x-ord.)	4	25	0.33	0.112	**10**	**26**	**0.38**	**0.053**	7	*0.68*	*0.090*	**7**	**0.77**	**0.041**
Rank ab. dist. sim. (RAD_D, MDS x-ord.)	4	25	0.33	0.110	9	26	0.31	0.127	7	*0.68*	*0.094*	**7**	**0.86**	**0.014**
Total ab. (TA_D, ind. grab^{-1})	*4*	*25*	*0.38*	*0.059*	9	26	0.36	0.074	7	0.57	0.180	**7**	**0.93**	**0.003**
Phylum density (ind. grab^{-1})														
Nematoda	4	25	0.31	0.135	9	26	0.24	0.246	7	−0.04	0.939	*7*	*0.68*	*0.094*
Arthropoda	**3**	*25*	**0.41**	**0.040**	**9**	*26*	**0.49**	**0.011**	**7**	**0.75**	**0.052**	7	0.54	0.215
Annelida	*3*	25	*0.35*	*0.090*	**9**	*26*	**0.46**	**0.019**	7	0.54	0.215	**7**	**0.82**	**0.023**
Nemertina	4	25	−0.28	0.178	*9*	*26*	−0.35	*0.079*	7	−0.07	0.879	7	0.21	0.645
Biomass-based														
Phyla comp. sim. (PC_B, MDS x-ord.)	**7**	**21**	**0.45**	**0.040**	10	22	0.32	0.151	6	0.46	0.354	6	0.58	0.228
Rank ab. dist. sim. (RAD_B, MDS x-ord.)	**7**	**21**	**0.61**	**0.003**	13	22	0.27	0.219	**6**	**0.83**	**0.042**	6	0.71	0.111
Total ab. (TA_B, g·grab^{-1})	**8**	**21**	**0.61**	**0.004**	13	22	0.30	0.179	**6**	**0.83**	**0.042**	6	0.71	0.111
Phylum biomass (g grab^{-1}):														
Nematoda	**4**	**22**	**0.48**	**0.025**	5	22	0.30	0.182	6	0.03	0.957	6	0.31	0.544
Arthropoda	**7**	**21**	**0.62**	**0.003**	**8**	**22**	**0.48**	**0.025**	**6**	**0.89**	**0.019**	**6**	**1.00**	**0.000**
Annelida	*10*	*22*	*0.38*	*0.081*	15	22	0.33	0.139	6	0.26	0.623	6	0.26	0.623
Nemertina	**4**	**22**	**−0.43**	**0.044**	**9**	**22**	**−0.58**	**0.005**	6	0.09	0.872	6	−0.09	0.872

Marginal ($0.05 < P \leq 0.10$) correlations are shown in italics and significant links are in boldface type ($P \leq 0.05$). The yearly density correlations have no lag and the biomass correlations were done with a year lag between environment or resource change and community change in accordance with the longer temporal lags noted in the monthly biomass-based correlations.

tance of existing individuals increasing substantially in size. Correspondence between the yearly TA_D and TA_B, PC_D and PC_B, and RAD_D and RAD_B is more evident (Fig. 3 A and B), but there are also periods such as 1996 when the association is still weak.

Year-to-year estimates of the POC inputs vs. SCOC rates have shown that there can be significant imbalances between food supply and demand (27, 30), but the analysis here found that increases in POC flux were still linked to increases in SCOC rates at Sta. M over both monthly ($n = 27$, $r_s = 0.55$, $P < 0.01$) and yearly ($n = 7$, $r_s = 0.75$, $P = 0.05$) scales. These links between POC flux and SCOC provide temporal perspective to spatial studies in the equatorial Pacific, which found increased SCOC below areas of higher POC flux (31). Multiple regressions were also used to evaluate whether SCOC could be estimated from POC flux and NOI inputs. Monthly regression could explain ~47% of the SCOC variability ($P < 0.001$) and 59% with yearly regressions, but without significance ($P > 0.05$).

None of the six macrofauna community parameters were significantly correlated to SCOC over seasonal or interannual scales. Studies of the remineralization of organic matter at the seafloor found that SCOC can have seasonal variations (27, 30) as do the macrofauna (22). The extent of the unexplained variation in the metazoan macrofauna vs. SCOC correlations over the 10-year period, however, suggests that seafloor respiration was significantly influenced by other biota including the microbial, meiofaunal, and protist portions of the sediment community. And, the macrofauna may integrate POC flux inputs over longer timescales than SCOC. Observational studies at other sites in the N Atlantic have found that increases in POC fluxes resulted in greater microbial activity and SCOC within weeks (32–34) with few exceptions (34, 35). Experimental additions of isotopically labeled POC were followed after 36 h with greater microbial biomass and synoptically increasing SCOC when compared to controls at (36) abyssal, as well as bathyal depths (37).

If SCOC is driven principally by other portions of the sediment community, then the dominant biogeochemical role of the metazoan macrofauna would principally be sediment mixing and organic matter repackaging rather than the transformation of organic carbon to CO_2 via respiration. A short-term study at Sta. M demonstrated that abyssal benthic metazoan macrofauna can ingest phytodetritus and mix labeled material down to a 5-cm depth in the sediment within 36 h (38). Likewise studies at other slope-to-abyssal sites have revealed mixing to a several-centimeter depth over periods of hours to days (39, 40). Mixing, which can move fresher organic matter and oxygen deeper into the sediment, could be an important mechanism of facilitation across faunal sizes (41). For example, greater sediment fauna diversity has been linked to greater ratios of benthic biomass to organic carbon inputs from slope-to-abyssal depths (42). Given the links between climate, POC flux, and macrofauna and mobile megafauna community structure variables, levels of bioturbation, facilitation, and burial are likely to vary as well. Radiotracer experiments in the equatorial Pacific did find that areas experiencing higher fluxes had higher bioturbation rates (40) with mixing to a several-centimeter depth.

Processes linking surface conditions to long-term metazoan macrofauna community dynamics likely extend to less productive waters, but relatively little temporal macrofauna data are available at other locations. Metazoan TA_D and TA_B, and SCOC were studied at an oligotrophic central north Pacific site (Station ALOHA, 22°145′N, 158°00′W, 4,730-m depth) over a 14-month period from December 1997 to January 1999 using techniques identical to those at Sta. M (23). The ALOHA benthic community study was supplemented by abyssal POC flux and primary production data from the HOT program operating synoptically at the site (43). Results from previous analysis of data from the site have shown that POC flux to a 4000-m depth (or
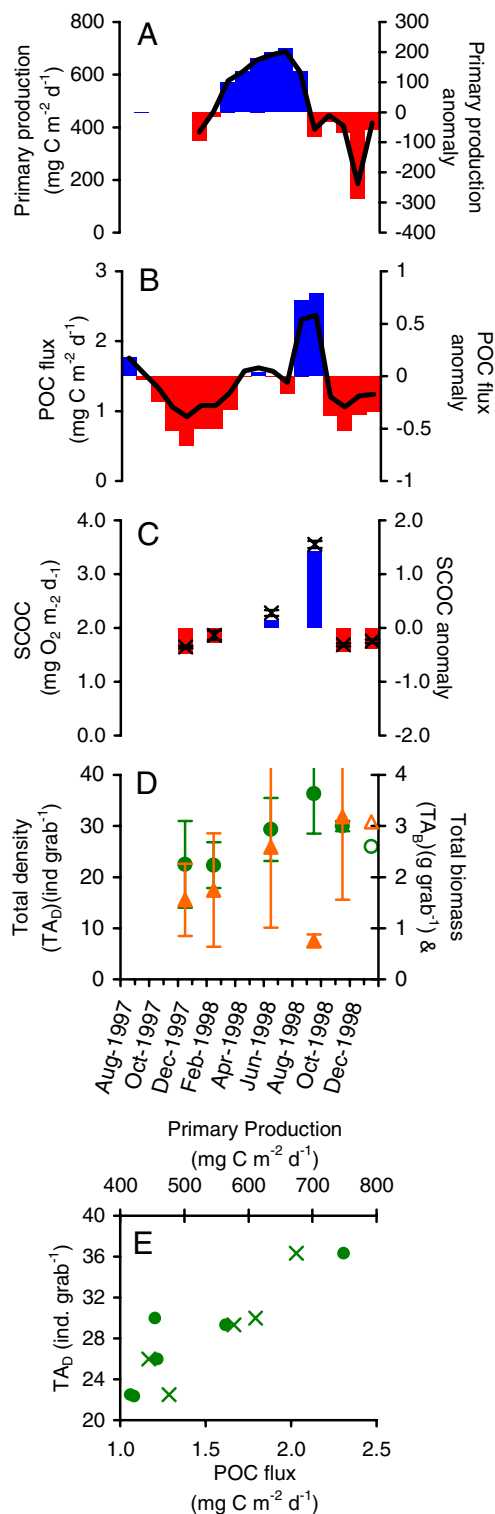
ECOLOGY

Fig. 4. Results from Sta. ALOHA illustrating monthly (*A*) sampled primary production (PP) at the surface (solid line) and its anomaly in blue and red bars; (*B*) POC flux to 4000 m (730 mab, solid line) and its anomaly in blue and red bars; (*C*) SCOC (×) and its anomaly in blue and red bars; (*D*) TA_D (circles) and TA_B (triangles) for total metazoan macrofauna with standard error bars, and (*E*) a TA_D during primary production and abyssal POC flux with temporal lags found in Table 1.

730 m above bottom) were correlated to SCOC with a lag of <14 days (Fig. 4 *A–C*) (23). Here, we found that measured TA_D had considerable correspondence to surface production ($n = 5$,

$r_s = 0.90$, $P = 0.04$) with a lag of 3 months and POC flux ($n = 6$, $r_s = 0.77$, $P = 0.07$) with a lag of 1 month (Fig. 4 *D* and *E*). The TA_B estimates followed the same trend with one major outlier. The coupling observed at ALOHA illustrates how metazoan macrofauna and carbon remineralization dynamics are related to surface conditions in oligotrophic regions, and higher productivity regions such as the California Current (Sta. M).

The correlations and regressions presented are site specific, limited to a span of 10 years, and of varied significance, but they represent a critical step toward quantifying seafloor community dynamics with more temporal context. Paleoecological research has suggested that climate-driven community collapses in the deep sea have occurred within the past several thousand years (20), but the research presented here shows that climate and resource forcing can lead to significant ($P < 0.05$) reductions in macrofauna abundance by one half in ~1 year along with shifts in composition, equitability, and size structure even at coarse taxonomic levels.

Our results demonstrate how broad community changes can be correlated to a varying resource and not a likely outcome of random ecological drift. A mosaic of nonequilibrium influences dominated by POC flux variation has been hypothesized to play a role in maintaining the diverse composition of deep-sea communities in both space and time (44). Community change can occur, in part, through differential responses between taxa to environmental and resource variables and competitive interactions. Enrichment experiments at Sta. M, and several other sites, have revealed that different portions of the macrofauna community have differential feeding morphology, behaviors, and thus responses in terms of their selection and uptake of labeled POC (36–38). Evidence for the differential utilization of resources has also been found in the mobile epibenthic megafauna (29). Clear evidence of links between variation in resources and community change has major importance for understanding what controls both marine and terrestrial biodiversity (45, 46) and longer-term biogeochemical cycling on Earth. Considering that the influence of food availability on the macrobenthos in the deep sea has been shown on broad spatial and temporal scales (10–18, 21–24, 36–40, 44, 47) the remaining challenge of developing informative estimations of future seafloor conditions from surface ocean conditions seems tractable.

Particulates that sink into the deep sea are effectively removed from surface systems for decades or more, but the fate of that sinking material can feedback to global biogeochemistry in the longer term. Our results specifically indicate that POC flux is positively correlated to total abundance, and significant increases in POC flux could lead to broad changes in metazoan macrofauna community structure including increased dominance of larger taxa, decreased equitability, and increased dissolved O_2 uptake and release of CO_2 during respiration.

Both proposed ocean-fertilization methods of carbon sequestration and secular climate change could have major impacts on deep-sea life with poorly understood biogeochemical feedbacks. If ocean iron fertilization efforts are successful in increasing net surface production and organic matter export into the deep sea, then clearly those large-scale anthropogenic changes in abyssal POC flux will also likely influence abyssal communities. Most evaluations of global climate change have understandably focused on affects likely to occur in the coming decades (48). Climate change is already implicated in significant alterations of oceanographic conditions worldwide (1, 2, 4, 6). Even global climate model scenarios that assume significantly reduced greenhouse gas emissions through societal change and technological advancements indicate that warming alone will likely continue through the year 2300 (48). Because impacts of abyssal community change are so poorly constrained in future projections, centennial-scale estimates may neglect feedbacks from the deep sea. Current estimates of

replacement times for deep-water masses below a 1,500-m depth, however, range from 85 to 889 years depending on the estimate assumptions and ocean basin (50–53). Therefore persistent changes in deep-seafloor processes could emerge in surface conditions and ultimately biogeochemical cycling within centennial scales.

1. Feely RA, et al. (2004) Impact of anthropogenic CO_2 on the $CaCO_3$ system in the oceans. Science 305:362–366.
2. Barnett TP, et al. (2005) Penetration of human-induced warming into the world's oceans. Science 309:284–287.
3. Pierce DW (2004) Future changes in biological activity in the North Pacific due to anthropogenic forcing of the physical environment. Climate Change 62:389–418.
4. Sabine CL, et al. (2004) The oceanic sink for anthropogenic CO_2. Science 305:367–371.
5. Behrenfeld MJ, et al. (2006) Climate-driven trends in contemporary ocean productivity. Nature 444:752–755.
6. Polovina JJ, Howell EA, Abecassis M (2008) Ocean's least productive waters are expanding. Geophys Res Lett 35: doi:10.1029/2007GL031745.
7. Bopp L, Aumont O, Cadule P, Alvain S, Gehlen M (2005) Response of diatoms distribution to global warming and potential implications: A global model study. Geophys Res Lett 32: doi:10.1029/2005GL023653.
8. Buesseler KO, et al. (2008) Ocean iron fertilization: Moving forward in a sea of uncertainty. Science 319:162.
9. Boyd PW, et al. (2007) Mesoscale iron enrichment experiments 1993–2005: Synthesis and future directions. Science 315:612–617.
10. Smith CR, et al. (1997) Latitudinal variations in benthic processes in the abyssal equatorial Pacific: Control by biogenic particle flux. Deep-Sea Res II 44:2295–2317.
11. Levin L, et al. (2001) Environmental influences on regional deep-sea species diversity. Annu Rev Ecol Syst 32:51–93.
12. Rex MA, et al. (2006) Global bathymetric patterns of standing stock and body size in the deep-sea benthos. Mar Ecol Prog Ser 317:1–8.
13. Johnson NA, et al. (2007) The relationship between the standing stock of deep-sea macrobenthos and surface production in the western North Atlantic. Deep-Sea Res I 54:1350–1360.
14. Rowe GT, Polloni PT, Haedrich RL (1982) The deep-sea macrobenthos on the continental margin of the northwest Atlantic Ocean. Deep-Sea Res A 29:257–278.
15. Cosson N, Sibuet M, Galéron J (1997) Community structure and spatial heterogeneity of the deep-sea macrofauna at 3 contrasting stations in the tropical northeast Atlantic. Deep-Sea Res I 44:247–269.
16. Gambi C, Danovaro R (2006) A multiple-scale analysis of metazoan meiofaunal distribution in the deep Mediterranean Sea. Deep-Sea Res I 53:1117–1134.
17. Thiel H, (1975) The size structure of the deep-sea benthos. Hydrobiol 60:576–606.
18. Kaariainen J, Bett BJ (2006) Evidence for benthic body size miniaturization in the deep sea. J Mar Biol Ass UK 86:1339–1345.
19. Cronin TM, Raymo ME (1997) Orbital forcing of deep-sea benthic species diversity. Nature 385:624–627.
20. Yasuhara M, Cronin TM, deMenocal PB, Okahashi H, Linsley BK (2008) Abrupt climate change and collapse of deep-sea ecosystems. Proc Natl Acad Sci USA 105:1556–1560.
21. Galéron J, et al. (2001) Temporal patterns among meiofauna and macrofauna taxa related to changes in sediment geochemistry at an abyssal NE Atlantic site. Prog Oceanog 50:303–324.
22. Drazen JC, Baldwin RJ, Smith KL, Jr. (1998) Sediment community response to a temporally varying food supply at an abyssal station in the NE Pacific. Deep-Sea Res II 45:893–913.
23. Smith KL, Jr., Baldwin RJ, Karl DM, Boetius A (2002) Benthic community responses to pulses in pelagic food supply: North Pacific subtropical gyre. Deep-Sea Res I 49:971–990.
24. Gooday AJ (1988) A response by benthic foraminifera to the deposition of phytodetritus in the deep sea. Nature 332:70–73.
25. Schwing FB, Murphree TP, Green M (2002) The evolution of oceanic and atmospheric anomalies in the northeast Pacific during the El Niño and La Niña events of 1995–2001. Prog Oceanog 53:115.
26. Smith KL, Jr., et al. (2006) Climate effect on food supply to depths greater than 4000 meters in the northeast Pacific. Limnol Oceanog 51:166.
27. Smith KL, Jr., Kaufmann RS, Baldwin RJ, Carlucci AF (2001) Pelagic-benthic coupling in the abyssal eastern North Pacific: An 8-year time-series study of food supply and demand. Limnol Oceanog 46:543–556.
28. Ruhl HA, Smith KL, Jr. (2004) Shifts in deep-sea community structure linked to climate and food supply. Science 305:513–515.
29. Ruhl HA (2008) Community change in the variable resource habitat of the abyssal northeast Pacific. Ecology 89:991–1000.
30. Smith KL, Jr., Kaufmann RS (1999) Long-term discrepancy between food supply and demand in the deep eastern North Atlantic. Science 284:1174–1177.
31. Berelson W (1997) Biogenic budgets of rain, benthic remineralization, and sediment accumulation in the equatorial Pacific. Deep-Sea Res II 44:2251–2282.
32. Graf G (1989) Benthic-pelagic coupling in a deep-sea benthic community. Nature 341:437–439.
33. Pfannkuche O (1993) Benthic response to the sedimentation of particulate organic matter at the BIOTRANS station, 47°N, 20°W. Deep-Sea Res II 40:135–149.
34. Pfannkuche O, Boetius A, Lochte K, Lundgreen U, Thiel H (1999) Responses of deep-sea benthos to sedimentation patterns in the North-East Atlantic in 1992. Deep-Sea Res I 46:573–596.
35. Sayles FL, Martin WR, Deuser WG (1994) Response of benthic oxygen demand to particulate organic carbon supply in the deep sea near Bermuda. Nature 371:686–689.
36. Witte U, et al. (2003) In situ experimental evidence of the fate of a phytodetritus pulse at the abyssal sea floor. Nature 424:763–766.
37. Witte U, Aberle N, Sand M, Wenzhöfer F (2003) Rapid response of a deep-sea benthic community to POM enrichment: An in situ experimental study. Mar Ecol Prog Ser 251:27–36.
38. Sweetman AK, Witte U (2008) Macrofaunal community composition, food web structure and short-term response to a simulated phytodetrital pulse in the abyssal northeast Pacific Ocean. Mar Ecol Prog Ser 355:73–84.
39. Levin LA, et al. (1999) Macrofaunal processing of phytodetritus at two sites on the Carolina margin: In situ experiments using ^{13}C-labeled diatoms. Mar Ecol Prog Ser 182:37–54.
40. Pope RH, Demaster DJ, Smith CR, Seltmann H (1996) Rapid bioturbation in equatorial Pacific sediments: Evidence from excess ^{234}Th measurements. Deep-Sea Res II 43:1339–1364.
41. Thistle D, Eckman JE, Paterson GLJ (2008) Large, motile epifauna interact strongly with harpactacoid copepods and polychaetes at bathyal site. Deep-Sea Res I 55:324–331.
42. Danovaro R, et al. (2008) Exponential decline of deep-sea ecosystem functioning linked to benthic biodiversity loss. Curr Biol 18:1–8.
43. Karl DM, Lukas R (1996) The Hawaii Ocean time-series (HOT) program: Background, rationale and field implementation. Deep-Sea Res II 43:129–156.
44. Grassle JF (1989) Species diversity in deep-sea communities. TREE 4:12–15.
45. Thibault KM, White EP, Ernest SKM (2004) Temporal dynamics in the structure and composition of a desert rodent community. Ecology 85:2649–2655.
46. Sugihara G, Bersier L-F, Southwood TR, Pimm SL, May RM (2003) Predicted correspondence between species abundances and dendrograms of niche similarities. Proc Natl Acad Sci USA 100:5246–5251.
47. Gooday AJ (2002) Biological responses to seasonally varying fluxes of organic matter to the ocean floor: A review. J Oceanog 58:305–322.
48. Intergovernmental Panel on Climate Change (2007) Climate change 2007: The physical science basis. Contribution of Working Group I to the Fourth Assessment Report of the Intergovernmental Panel on Climate Change, eds Solomon S, et al. (Cambridge Univ Press, Cambridge, UK).
49. Stuiver M, Quay PD, Ostlund HG (1983) Abyssal water carbon-14 distribution and the age of the world oceans. Science 219:849–851.
50. Broecker WS, et al. (1998) How much deep water is formed in the Southern Ocean? J Geophys Res 103(C8):15833–15844.
51. Sarmiento JL, Gruber N (2006) Ocean Biogeochemical Dynamics (Princeton Univ. Press, Princeton, NJ), p 503.
52. Matsumoto K (2008) Radiocarbon-based circulation age of the world oceans. J Geophys Res 112:C09004, doi:10.1029/2007JC004095.

ECOLOGY